SAN JOSÉ STATE UNIVERSITY

Impact of Material Properties on Bay Area Rupture Dynamics
2025 SCEC Annual Meeting

Ritwik Patil
Elizabeth Madden

Introduction

Northern California's Bay Area lies along the Pacific North American plate boundary, placing millions of residents at risk from damaging earthquakes. To investigate how large ruptures might evolve across this system, we model earthquake dynamics along the Calaveras, Hayward, and Rodgers Creek faults. These faults form a major hazard network, with the Rodgers Creek fault extending 45 km north of Santa Rosa and the Calaveras fault stretching 65 km south of Gilroy to its junction with the San Andreas fault. In our simulations, we compare scenarios with realistic versus simplified material properties to evaluate how subsurface structure influences rupture initiation, propagation, and fault interaction. Scan the QR code on the right to explore these faults directly on Google Maps.

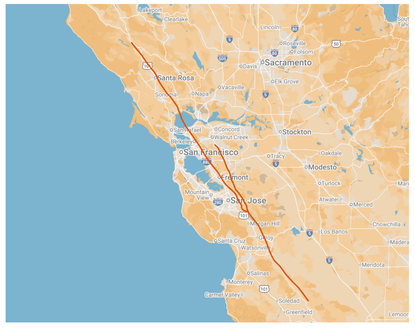

Figure 1: Fault system included in our model (map created using Google My Maps [1])

Method

We constructed a high resolution 3D structural model and tetrahedral mesh of the Rodgers Creek, Hayward, Calaveras, and Northern Calaveras faults using fault traces from the National Seismic Hazard Model [2], incorporating topographic elevation from the USGS 3D Elevation Program [3]. For dynamic rupture simulations, we use SeisSol [4], [5], an open-source code for earthquake modeling that implements the ADER-DG method.

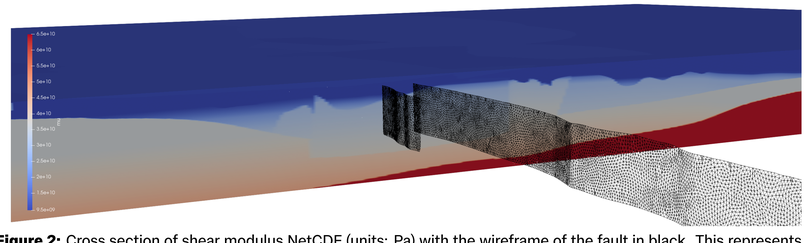

Figure 2: Cross section of shear modulus NetCDF (units: Pa) with the wireframe of the fault in black. This represents the realistic material properties model.

Each simulation is initialized with a static stress field of $\sigma_{xx} = 40.5$ MPa, $\sigma_{yy} = 40.5$ MPa, and $\sigma_{xy} = 20.5$ MPa. To include realistic material properties, we generated a NetCDF file containing density and Lamé's parameters λ and μ from the USGS 3D seismic velocity model for the San Francisco Bay region [6]. Fault failure is governed by a linear slip weakening friction law. All simulations were run on the Expanse supercomputer at the San Diego Supercomputer Center[7], using four nodes per run (128 CPU cores per node) with an average sustained performance of 2.45 TFLOP/s.

For the homogeneous case, we use $\rho = 2670\,\mathrm{kg\,m^{-3}}$, $\mu = 3.90 \times 10^{10}$ Pa, and $\lambda = 4.24 \times 10^{10}$ Pa, and we also impose minimum values of P-wave velocity $3600\,\mathrm{m\,s^{-1}}$, S-wave velocity $1950\,\mathrm{m\,s^{-1}}$, and density $2550\,\mathrm{kg\,m^{-3}}$ for the heterogeneous case, following Harris et al. [8].

Results

Rupture Time

When material properties are included, rupture propagation shows distinct differences compared to the homogeneous case. The rupture front does not extend as far south, halting near Gilroy, and it also takes longer to reach the northern extent near Santa Rosa. Although rupture expansion to the fault edges is slower overall, the transfer of rupture between fault segments occurs approximately 4 seconds earlier than in the homogeneous simulation.

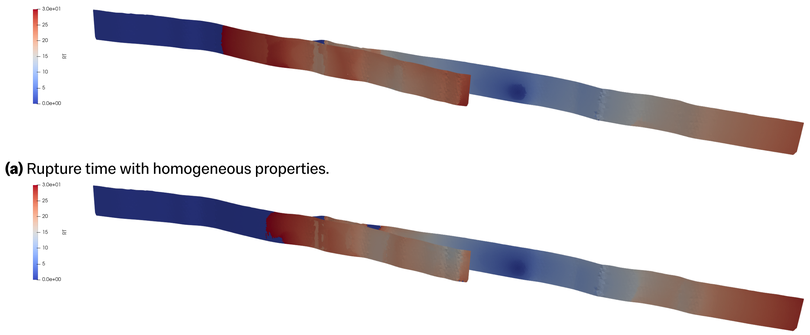

(a) Rupture time with homogeneous properties.

(b) Rupture time with heterogeneous properties.

Figure 3: Comparison of rupture time on the fault (units: s).

Energy

These differences in rupture evolution are also reflected in the overall energy release and fault mechanics. The seismic moment (M_0) grows more slowly in the heterogeneous case, consistent with delayed rupture propagation toward the northern and southern fault tips. For reference, the model with homogeneous material properties generates a M_w 7.65 event, while the heterogeneous properties result in a M_w 7.71 event. Additionally, the radiated energy (E_r) increased when realistic material properties are included, indicating that more elastic energy is emitted as seismic waves. Here E_r is calculated following Ma and Archuleta [9] as the difference between the total work (W_t) and the static work (W_s).

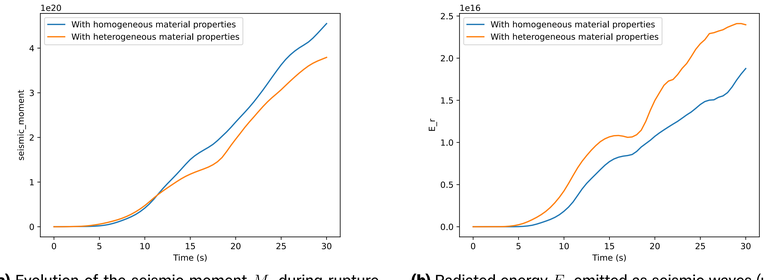

(a) Evolution of the seismic moment M_0 during rupture (units: N·m).

(b) Radiated energy E_r emitted as seismic waves (units: J).

Figure 4: Comparison of seismic moment and radiated energy in simulations with and without material property heterogeneity.

Slip and Displacement

Another key difference is observed in the accumulated slip distribution. When material properties are included, the accumulated slip near the surface is nearly doubled compared to the homogeneous case. This amplification is also reflected in the surface displacement, where certain regions experience significantly greater movement.

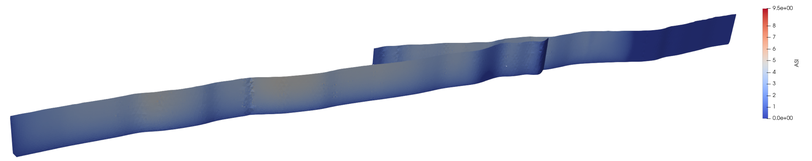

(a) With homogeneous properties.

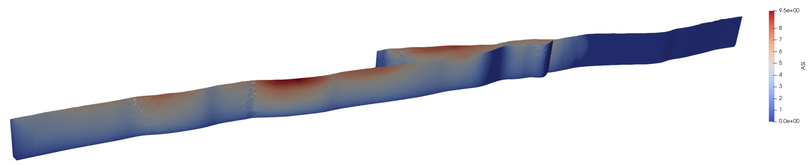

(b) With heterogeneous properties.

Figure 5: Comparison of accumulated slip (ASl) on the fault (units: m).

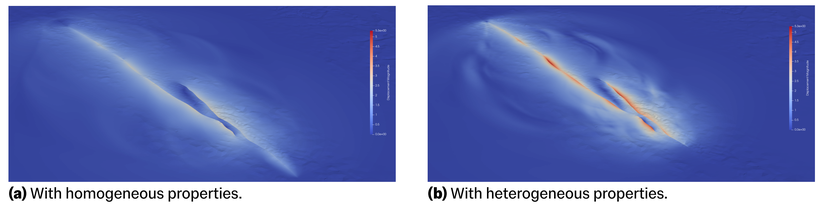

(a) With homogeneous properties.

(b) With heterogeneous properties.

Figure 6: Ground displacement magnitude (units: m).

Future Work

Potential next steps include investigating how rupture dynamics are affected by the intersection of the Calaveras and Hayward fault traces near San Felipe, and testing nucleation at different locations and depths to better understand their influence on slip and surface displacement.

References

[1] Google LLC, Google my maps, https://www.google.com/mymaps, Accessed: September 2, 2025, 2025.

[2] A. E. Hatem et al., "Simplifying complex fault data for systems-level analysis: Earthquake geology inputs for u.s. nshm 2023," Scientific Data, vol. 9, no. 1, Aug. 2022, ISSN: 2052-4463. DOI: 10.1038/s41597-022-01609-7 [Online]. Available: http://dx.doi.org/10.1038/s41597-022-01609-7

[3] The National Map—New data delivery homepage, advanced viewer, lidar visualization. 2019. DOI: 10.3133/fs20193032 [Online]. Available: http://dx.doi.org/10.3133/fs20193032

[4] C. Pelties, J. de la Puente, J.-P. Ampuero, G. B. Brietzke, and M. Käser, "Three-dimensional dynamic rupture simulation with a high-order discontinuous galerkin method on unstructured tetrahedral meshes," Journal of Geophysical Research: Solid Earth, vol. 117, no. B2, 2012. DOI: https://doi.org/10.1029/2011JB008857 eprint: https://agupubs.onlinelibrary.wiley.com/doi/pdf/10.1029/2011JB008857. [Online]. Available: https://agupubs.onlinelibrary.wiley.com/doi/abs/10.1029/2011JB008857

[5] A.-A. Gabriel et al., SeisSol. [Online]. Available: https://github.com/SeisSol/SeisSol

[6] B. T. Aagaard and E. T. Hirakawa, San francisco bay region 3d seismic velocity model v21.1, 2021. DOI: 10.5066/P9TRDCHE [Online]. Available: https://www.sciencebase.gov/catalog/item/61817394d34e9f2789e3c36c

[7] S. Strande et al., "Expanse: Computing without boundaries: Architecture, deployment, and early operations experiences of a supercomputer designed for the rapid evolution in science and engineering," in Practice and Experience in Advanced Research Computing 2021: Evolution Across All Dimensions, ser. PEARC '21, Boston, MA, USA: Association for Computing Machinery, 2021, ISBN: 9781450382922. DOI: 10.1145/3437359.3465588 [Online]. Available: https://doi.org/10.1145/3437359.3465588

[8] R. A. Harris et al., "A geology and geodesy based model of dynamic earthquake rupture on the rodgers creek-hayward-calaveras fault system, california," Journal of Geophysical Research: Solid Earth, vol. 126, no. 3, e2020JB020577, 2021, e2020JB020577 2020JB020577. DOI: https://doi.org/10.1029/2020JB020577 eprint: https://agupubs.onlinelibrary.wiley.com/doi/pdf/10.1029/2020JB020577. [Online]. Available: https://agupubs.onlinelibrary.wiley.com/doi/abs/10.1029/2020JB020577

[9] S. Ma and R. J. Archuleta, "Radiated seismic energy based on dynamic rupture models of faulting," Journal of Geophysical Research: Solid Earth, vol. 111, no. B5, 2006. DOI: https://doi.org/10.1029/2005JB004055 eprint: https://agupubs.onlinelibrary.wiley.com/doi/pdf/10.1029/2005JB004055. [Online]. Available: https://agupubs.onlinelibrary.wiley.com/doi/abs/10.1029/2005JB004055

Acknowledgments

1. National Science Foundation EMBRACE Program
2. SJSU RSCA Seed Grant Program
3. HPC resources provided through the NSF Access Program